

https://dspace.org/

Contrasting the effect of hige region insertions and nonactive site mutations on HIV proteaeinhibitor interactions Insights from altered flap dynamics

Tshele Mokhantso; Dean Sherry; Roland Worth; Ramesh Pandian; Ikechukwu Achilonu ...

https://hdl.handle.net/10539/40617
WOS

Downloaded from a DSpace repository. https://dspace.org/

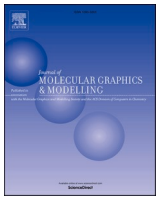
Journal of Molecular Graphics and Modelling 133 (2024) 108850



Contents lists available at ScienceDirect

Journal of Molecular Graphics and Modelling

journal homepage: www.elsevier.com/locate/jmgm



Contrasting the effect of hinge region insertions and non-active site mutations on HIV protease-inhibitor interactions: Insights from altered flap dynamics

Tshele Mokhantso, Dean Sherry, Roland Worth, Ramesh Pandian, Ikechukwu Achilonu, Yasien Sayed *

Protein Structure-Function Research Unit, School of Molecular and Cell Biology, University of the Witwatersrand, Johannesburg, 2050, South Africa

A B S T R A C T

HIV-1 protease (PR) enzyme is a viable antiretroviral drug target due to its crucial role in HIV maturation. Over many decades, the HIV-1 PR enzyme has exhibited mutations brought on by drug pressure and error-prone nature of HIV-1 reverse transcriptase. Non-active site mutations have played a pivotal role in drug resistance; however, their mechanism of action has not been fully elucidated. We investigated how non-active site mutations affect the conformational stability and drug binding ability of HIV-1 PR. In light of this, we studied a novel HIV-1 subtype C protease variant containing an insertion of valine (↑V) in the hinge region. We analysed the mutations in the presence and absence of ten background mutations. Molecular dynamics simulations revealed that both with and without the background mutations, the PR exhibited increased flexibility of hinge, flaps and fulcrum regions. This allowed the PR to adopt a wider flap conformation when in complex with several inhibitors. Additionally, the simulations revealed that the protease inhibitors (PIs) could not bring the mutated variant proteases into a stable, closed conformation, resulting in increased solvent exposure of the inhibitors. Together, these results suggest that the mutations decrease the favourability of binding by altering the dynamics of the flap regions. Notably, the insertion mutation increased PR hinge flexibility and the introduction of background mutations compensated for this by stabilising the cantilever and hinge regions. Together, these findings provide insight into how non-active site mutations affect PR conformational dynamics in critical areas of the PR thus impacting on drug binding capacity and potentially contributing to drug resistance.

1. Introduction

1.1. Human immunodeficiency virus

(HIV) protease (PR) plays a crucial role in the viral replication cycle and is a significant target for antiretroviral therapy [1]. While the use of antiretroviral drugs has led to significant improvements in the treatment and management of HIV infection, the development of drug resistance remains a significant challenge [2,3]. HIV protease inhibitors (PIs) have been used extensively in the treatment of HIV infection; however, the emergence of HIV-1 PR drug-resistance mutations presents a significant limitation to their long-term efficacy [4–6].

Resistance begins with genetic changes in the viral genome following exposure to antiretroviral drugs. Resistance starts with primary mutations that accumulate in the PR active site cavity. Primary mutations directly impact the protein drug interface in a manner that can significantly diminish binding affinity. However, primary resistance mutations can also deleteriously affect the ability of the PR to bind to and hydrolyse its natural Gag and Gag-Pol protein substrates. As such, secondary mutations tend to arise in regions distal to the active site cavity, leading to changes in the viral phenotype, including restoring standard or enhanced catalytic activity and resistance to PIs [7]. Secondary mutations in the PR are known to play a critical role in the development of drug resistance, and there is a growing body of research investigating the mechanisms underlying these mutations [8–11]. Secondary mutations can impact the conformational stability and activity of the PR [12,13] and can lead to changes in the dynamics of the enzyme in a manner that can compensate for the adverse effects of primary mutations on the protease activity and viral fitness [10,14].

The critical role that non-active site mutations play in resistance is evident when resistance to multiple PIs is associated with many non-active site mutations that augment the mechanism of one or two active site mutations [15]. Additionally, the effect of active site mutations on drug resistance is radically reduced when all the accompanying non-active site mutations are reverted to the corresponding wild-type residue. Indeed, non-active site mutations are thought to accumulate to re-stabilise enzyme activity, a phenomenon observed with oseltamivir resistance in influenza [16].

* Corresponding author.
E-mail address: yasien.sayed@wits.ac.za (Y. Sayed).

https://doi.org/10.1016/j.jmgm.2024.108850
Received 31 October 2023; Received in revised form 22 August 2024; Accepted 26 August 2024
Available online 29 August 2024
1093-3263/© 2024 The Authors. Published by Elsevier Inc. This is an open access article under the CC BY-NC license (http://creativecommons.org/licenses/by-nc/4.0/).

Although it is not fully understood how these non-active site mutations impart their effect, some explanation may lie in the effect on the conformational flexibility of mutant PRs [10]. Specifically, non-active site mutations are likely to affect the molecular dynamics of the flap regions of the PR by modulating the stability of other distinct regions of the PR, such as the cantilever, fulcrum and hinge regions. Changes in the dynamics of these regions have been shown to work cooperatively to influence the protein-drug interface [17–19]. Moreover, mutations and insertions located in the hinge region of the PR have been shown to affect drug susceptibility [10,20–23]. Therefore, understanding how insertions and mutations influence the conformational stability and function of HIV PR is critical to understanding how these non-active site mutations bring about drug resistance.

Globally, 47 % of the HIV cases are subtype C related, with only about 10 % belonging to subtype B (www.aidsmap.com). In Africa, HIV/AIDS accounts for more than 66 % of global cases and subtype C is the predominant subtype (UNAIDS, 2022). However, all antiretroviral therapy has for many decades focused on HIV-1 subtype B, with HIV-1 subtype C being relatively understudied and under-reported. Considering this, the current study is aimed at assessing how secondary background mutations outside the active site affect the conformational stability and drug binding of a novel HIV-1 subtype C protease variant using molecular dynamics simulations and molecular docking. This novel HIV subtype C PR variant contained an amino acid polymorphism at position 37 and a hinge region insertion (↑V) (Fig. 1). Furthermore, this PR variant contained ten additional background amino acid polymorphisms. In order to dissect the independent effects of these mutations on the dynamics of the PR, these mutations were investigated independently. The hinge region insertion was analysed with and without the ten additional background mutations.

2. Methods

2.1. Homology modelling

Four homology models (Fig. 1A) were constructed (N37T↑V, N37T↑V^{+10}, N37T and N37T^{+10}) to study the effect of non-active site mutations on the dynamics of the PR. The first PR model, termed N37T↑V contained a single substitution mutation (N37T) and an insertion of a valine at position 37 (↑V). The second PR model, N37T↑V^{+10} contained the same mutations present in N37T↑V but with the additional ten background mutations: I13V, G16E, I36T, P39S, D60E, Q61E, I62V, L63P, V77I and M89L. The third protease model contained a single substitution of asparagine to threonine at position 37. The fourth protease model contained the N37T substitution mutation with ten background mutations and no valine insertion. The homology models were constructed using the SWISS-MODEL online tool (Arnold et al., 2006) with the atomic coordinates of the wild-type (WT) PR (PDB ID: 3U71) as a template. The homology models were validated using PROCHECK [24]. The homology structures of the two variants showing the root-mean-square deviation (rmsd) between the template and the predicted structures was calculated to 0.058 Å and 0.097 Å for the N37T↑V and N37T↑V^{+10} HIV-1 PR variants, respectively. Fig. 1A (WT- N37T↑V) and Fig. 1B (WT- N37T↑V^{+10}).

2.2. Molecular docking

The induced-fit docking studies were performed using Glide software (Schrödinger LLC 2009, USA) implemented on Windows architecture. The protein preparation step involved using the Schrödinger modules Glide, Prime, and Protein Preparation Wizard (Schrödinger LLC 2009, USA). The two-dimensional chemical structures of nine HIV protease inhibitors (PIs) approved by the FDA were obtained from PubChem (https://pubchem.ncbi.nlm.nih.gov/); namely, Atazanavir (ATV, CID: 148192), Darunavir (DRV, CID: 213039), Fosamprenavir (FPV, CID: 131536), Indinavir (IDV, CID: 5462355), Lopinavir (LPV, CID: 92727), Nelfinavir (NFV, CID: 64142), Ritonavir (RTV, CID: 392622), Saquinavir (SQV, CID: 60787) and Tipranavir (TPV, CID: 54682461). The LigPrep tool (Schrödinger LLC 2009, USA) was used to convert the ligand structures from two-dimensional into three-dimensional structures by adding hydrogens, bond angles, and lengths, choosing the correct chirality, and performing energy minimisation. The Epik tool selected the lowest energy tautomers and ring structures. Energy-minimised WT PR, N37T↑V PR, and N37T↑V^{+10} PR were docked with each of the nine PIs by defining the active site Asp25 residues as the centre of the docking region. The induced-fit docking was performed using the OPLS3 force field. The van der Waals radii of non-polar atoms of the PRs were scaled by a factor of 0.50, and 20 conformational poses were calculated for each complex. The docking score, Glide energy, and Glide E-model were used to choose the best conformation for further analyses using

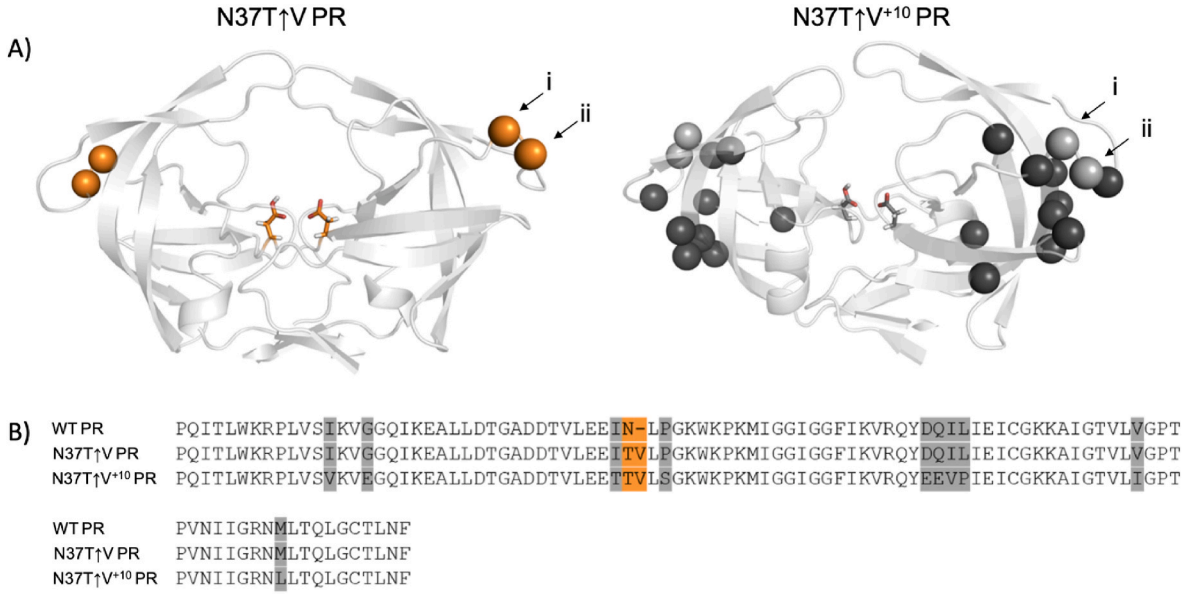


Fig. 1. A) Ribbon representation of N37T↑V PR (left) and N37T↑V^{+10} PR (right) and B) Amino acid sequence alignment of the WT subtype C PR, N37T↑V PR and N37T↑V^{+10} HIV PR. The arrows indicate (i) the N37T substitution and (ii) insertion mutations present in N37T↑V. The ten background mutations present in N37T↑V^{+10} are represented in dark grey. The Asp25/25′ catalytic residues are represented as sticks.

molecular dynamics simulations. Hydrophobic interactions and hydrogen bonds formed between each ligand and each protease were visualised using LigPlot+.

2.3. MM/GBSA binding energy calculation

The grid files for the three HIV-1 protease structures were constructed using the receptor grid generation panel of the Glide module in Maestro. A centroid of the prepared protein residues was selected to generate a grid box. A partial atomic cut off of 0.25 with 1.00 Å van der Waals radius scaling factor was selected to generate the receptor grid box using the OPLS2005 force field. The library of HIV-1 PIs was docked to the receptors using the virtual screening workflow of the Glide module in Maestro. This was followed by more rigorous and extensive screening using the standard precision (SP) and extended precision (XP) mode of Glide Maestro, which uses more complex sampling and scoring functions to penalise compounds exhibiting weak binding affinity in the protein cavity. The prime Molecular Mechanics-Generalised Born Surface Area (MM-GBSA) module was used to post-process the poses of the docked ligands for rescoring in order to obtain the binding energies. The binding free energy (ΔG_{bind}) was calculated from the equation below:

$$\Delta G_{bind} = \Delta G_{complex} - \Delta G_{protein} - \Delta G_{ligand}$$

$\Delta G_{complex}$, $\Delta G_{protein}$, and ΔG_{ligand} represent the free energy of the optimised protein-ligand complex, the free protein receptor, and the free ligand, respectively.

2.4. Molecular dynamics simulations

Molecular dynamics (MD) simulation studies were performed using Desmond software version 11.2 (Schrödinger LLC 2009, USA) using the OPLS3 force field for all the PR systems. The simulations were conducted with explicit solvent generated using the TIP3P solvation model within the System Builder module. The solvated systems were subjected to relaxation and minimisation using the steepest descent method until the system reached an atomic force of less than 100 kJ mol^{-1} nm^{-1}. This process performs a series of minimisations and short MD simulations to equilibrate each system before the experimental simulation commences. Briefly, a 5 ns MD simulation is performed under the NVT ensemble (constant number of particles (N), constant volume (V) and constant temperature (T)). After that, a 5 ns simulation is performed under the NPT ensemble (constant number of particles (N), constant pressure (P) and constant temperature (T)) at a temperature of 10 K and a pressure of 1 atm. Following equilibration, the MD simulations were performed for 200 ns at a constant temperature of 300 K with a Berendsen thermostat and an average pressure of 1 atm maintained by the Parrinello-Rahman barostat algorithm [25].

2.5. Computational data acquisition

The quality of the trajectories was assessed using the Simulation Quality Analysis Module in Maestro (Maestro 13.0, Schrödinger, 2021). The trajectory analyses such as atomic root-mean-square deviation (RMSD), root-mean-square fluctuation (RMSF), ligand interaction diagrams, solvent accessible surface area (SASA) and radius of gyration (R_g) were performed using the Simulation Event Analysis and Simulation Interaction Diagram modules in Maestro. The simulation trajectories were visualised and analysed using UCSF Chimera version 1.11.2 and PyMOL (The PyMOL Molecular Graphics System, Version 1.8 Schrödinger, LLC.). Sequence alignments were performed using the Clustal Omega tool (EMBL-EBI).

3. Results and discussion

3.1. Non-active site mutations in N37T↑V PR and N37T↑V^{+10} PR reduce the predicted binding affinity of PIs

Induced-fit docking (IFD) was used to systematically predict the interactions between the PR variants and nine FDA-approved PIs utilised in this study. The calculated free energy score (G_{score}) approximates the binding affinity of each protease variant for the nine PIs (Table 1 and Table S1). A negative binding energy typically indicates a favourable binding interaction between a protein target and an inhibitor, indicating that the molecules are more energetically stable when bound than when they are apart. All inhibitors exhibited negative binding free energies for the WT PR, N37T↑V, and N37T↑V^{+10} PR variants. However, the binding efficiency varied significantly when comparing the WT and mutated PR variants. Notably, the calculated G_{score} was not significantly different between the three PRs when in complex with IDV, LPV, and SQV. In contrast, the calculated G_{score} for the PRs in complex with ATV, DRV, FPV, NFV, RTV, and TPV exhibited marked decreases when in complex with N37T↑V PR and N37T↑V^{+10} PR (Table 1). The observed decrease in the G_{score} suggests these PIs may bind the PR mutants less effectively. As such, these complexes were selected for further analyses by MD simulations since IFD is limited to a static representation of the inherently dynamic complexes.

3.2. van der Waals interactions predominantly drive protease inhibitor binding

We explored the binding affinities of various PIs to the WT, N37T↑V, and N37T↑V^{+10} HIV-1 PRs. Notably, the mutants harbour insertion mutations in the flap hinges, potentially altering the protein's architecture, leading to increased dynamics and wider flap opening. These structural changes can affect the accessibility and conformational flexibility of the active site, consequently impacting on the drug binding affinity of each ligand. In Table 2, the binding affinities of the various PIs to WT, N37T↑V and N37T↑V^{+10} are presented. Saquinavir has the highest binding affinity when bound to all three PRs and is indicative of robust interactions with the HIV-1 PRs (ΔG_{bind} = −56.22 kcal/mol for WT, −55.56 kcal/mol for N37T↑V, and −63.38 kcal/mol for N37T↑V^{+10}). Ritonavir also displayed notable binding affinity across all PRs (ΔG_{bind} = −55.63 kcal/mol for WT, −47.87 kcal/mol for N37T↑V, and −49.33 kcal/mol for N37T↑V^{+10}).

van der Waals interactions contributed predominantly to the binding for most PIs, which is consistent with previous findings [45–47] and describes the geometry, chemical features, and ligand binding mode at

Table 1
Summary of G_{score} of nine FDA-approved PIs in complex with WT PR, N37T↑V PR and N37T↑V^{+10} PR.

Glide score (G_{score})			
Protease inhibitor	Wild-Type	N37T↑V	N37T↑V^{+10}
ATV	-12.20	-11.15	-10.32
DRV	-7.26	-7.65	-8.61
FPV	-8.26	-10.01	-9.18
IDV	-11.36	-11.68	-11.09
LPV	-11.10	-11.33	-10.49
NFV	-8.74	-9.86	-9.37
RTV	-12.20	-12.10	-10.80
SQV	-12.25	-12.19	-12.23
TPV	-9.60	-10.63	-8.57

Table 2
Binding affinities of protease inhibitors to WT, N37T↑V, and N37T↑V^{+10} HIV-1 PRs.

Receptors	PI	ΔG_{Bind}	ΔG_{Elec}	ΔG_{Cov}	ΔG_{HB}	ΔG_{Lipo}	ΔG_{Sol}	ΔG_{vDw}
WT	Amprenavir	−42.44	−8.25	5.81	−1.93	−15.23	16.14	−38.98
	Darunavir	−28.72	1.71	−0.33	−2.48	−11.24	17.11	−33.49
	Indinavir	−54.90	9.81	5.15	−2.18	−19.81	4.41	−51.65
	Indinavir sulfate	−54.90	9.81	5.15	−2.18	−19.81	4.41	−51.65
	Lopinavir	−34.64	−0.04	0.89	−0.27	−20.83	35.68	−48.59
	Nelfinavir	−26.84	−2.41	0.20	−9.81	4.72	−11.10	−20.43
	Ritonavir	−55.63	−9.50	2.92	−0.68	−22.51	32.93	−58.57
	Saquinavir	−56.22	16.29	4.80	−1.34	−21.91	2.27	−56.29
	Tipranavir	−39.96	−8.59	4.67	−0.59	−15.45	24.56	−44.05
N37TV	Atazanavir	−40.75	0.38	4.16	−0.88	−18.59	32.22	−56.42
	Darunavir	−36.11	−1.16	3.17	−2.75	−14.50	18.10	−38.98
	Fosamprenavir	−33.66	0.99	5.61	−2.32	−10.72	13.07	−40.30
	Indinavir	−54.10	8.35	5.50	−1.74	−20.15	5.28	−50.58
	Indinavir sulfate	−54.10	8.35	5.50	−1.74	−20.15	5.28	−50.58
	Nelfinavir	−39.02	19.76	3.19	−1.33	−18.07	3.83	−46.18
	Ritonavir	−47.87	−5.43	2.86	−0.23	−22.74	36.17	−57.21
	Saquinavir	−55.56	8.31	8.55	−1.72	−21.92	7.59	−56.35
	Tipranavir	−41.02	−3.31	4.59	−0.40	−15.98	22.37	−47.10
N37TV_BM	Amprenavir	−47.92	−0.19	8.01	−0.87	−17.81	6.77	−43.85
	Atazanavir	−37.95	−12.46	11.44	−1.17	−21.06	33.65	−48.34
	Darunavir	−37.48	−8.69	6.80	−1.17	−17.20	17.44	−34.65
	Fosamprenavir	−23.61	8.08	6.33	−1.24	−11.73	7.96	−33.01
	Indinavir	−53.18	12.01	5.67	−1.54	−20.18	0.84	−49.20
	Indinavir sulfate	−53.20	11.76	5.50	−1.50	−20.33	1.34	−49.18
	Lopinavir	−40.20	0.07	4.47	−0.15	−19.34	23.38	−47.81
	Nelfinavir	−33.15	30.68	7.24	−0.35	−19.62	−8.32	−42.78
	Ritonavir	−49.33	−15.28	5.47	−1.34	−21.81	42.08	−57.06
	Saquinavir	−63.38	6.60	1.05	−1.38	−20.75	5.50	−52.82
	Tipranavir	−41.54	−1.19	1.04	−0.36	−15.39	17.09	−42.73

the active site [46]. This also further confirmed the overall hydrophobic nature of the active site as a result of hydrophobic residues in the binding pocket. Additionally, electrostatic interactions (ΔG_{ele}), lipophilic interactions (ΔG_{lipo}), and solvation energy (ΔG_{sol}) played significant roles in shaping the binding energy landscape. The mutations likely influenced the openness of the flaps, altering the hydrophobic pocket thereby impacting ligand accessibility and the nature of ligand-protein interactions. Nelfinavir exhibited distinct binding affinities for WT (−26.84 kcal/mol), N37T↑V (−39.02 kcal/mol), and N37T↑V^{+10} (−33.15 kcal/mol), suggesting alterations in binding modes and dynamics induced by the mutations. Atazanavir, with ΔG_{bind} values of −40.75 kcal/mol for WT, −37.95 kcal/mol for N37T↑V, and −48.34 kcal/mol for N37T↑V^{+10}, also displayed varied affinities, indicating potential sensitivity to structural changes induced by the mutations. However, other PIs such as Darunavir, Fosamprenavir, and Tipranavir showed less pronounced variations in binding affinities across the protease variants, suggesting a certain level of resilience to structural alterations in the protease. Understanding the differential responses of wild-type and mutant forms of HIV-1 PR to PIs is crucial for rational drug design and the development of effective antiretroviral therapies. PIs with higher binding affinities, such as Saquinavir and Ritonavir, may hold promise for further development. However, the varied responses of PIs to structural alterations in the protease highlight the need for tailored therapeutic strategies to address drug resistance mechanisms.

3.3. Individual non-active site polymorphisms have varying impacts on the binding affinity of several PIs

In order to gain further insight into the contribution of each background mutation to changes in the predicted affinity, we analysed the effect reverting each mutation would have on the G_{score} while retaining the other nine background mutations. The analyses show that S39 consistently provides the most significant change in the calculated G_{score} when reverted to the wild-type proline residue (Fig. S1). The P39S mutation occurs in the hinge region of the PR, and substituting proline for a more flexible serine residue may increase the mobility of this region in a manner that affects the flaps during binding. Future studies could be directed towards investigating the role that proline plays in the dynamics of this region. To a lesser extent, reversion of I13V, V77I and M89L mutations significantly improved the calculated binding affinity of ATV, DRV, and TPV (Fig. S1). Notably, it has been shown that I13V and V77I mutations play a role in increased flap and hinge region dynamics, resulting in the PR favouring the semi-open conformation when in complex with these inhibitors [18]. Constellations of non-active site mutations are required to reach high levels of drug resistance in the HIV-1 PR. However, it is important to consider the contribution of individual or smaller sets of mutations and how these contribute cooperatively to drug resistance mechanisms.

3.4. N37T↑V PR and N37T↑V^{+10} PR sample wider flap conformations for extended periods

Flap tip curling is understood to promote flap opening in the HIV-1 PR [26]. Therefore, both phenomena were analysed to determine the effect of non-active site mutations on flap tip curling and flap dynamics. The angle between the adjacent alpha carbons (C_α) of the flap tips (Gly-49, Ile-50, and Gly-51) has been widely used as a metric to measure flap tip curling in HIV-1 protease [27] where the flap tips are considered curled in and curled out when the angle between the adjacent alpha carbons is ~100° and ~140°, respectively. Additionally, the interatomic distance between Cα atoms of Asp-25 and Ile-50 have been used to define the closed, semi-open and fully open flap conformations as <17 Å, 17–22 Å and >22 A, respectively [18,28]. It should be noted that the hinge insertion in both mutant PRs increased the residue numbering by one, which was considered during analysis.

In the apo monomer A (Fig. 2), the flap remains in the closed position during the entire simulation for WT while the mutants exhibit a relatively wider flap conformation in the semi-open range. With regards to monomer B, all three PRs remain largely in the closed conformation. In the apo monomer A (Fig. 2), the flap tip of the WT PR samples a larger angle of ~140° (curling out) which is directly correlated with the monomer adopting a closed flap conformation with an average

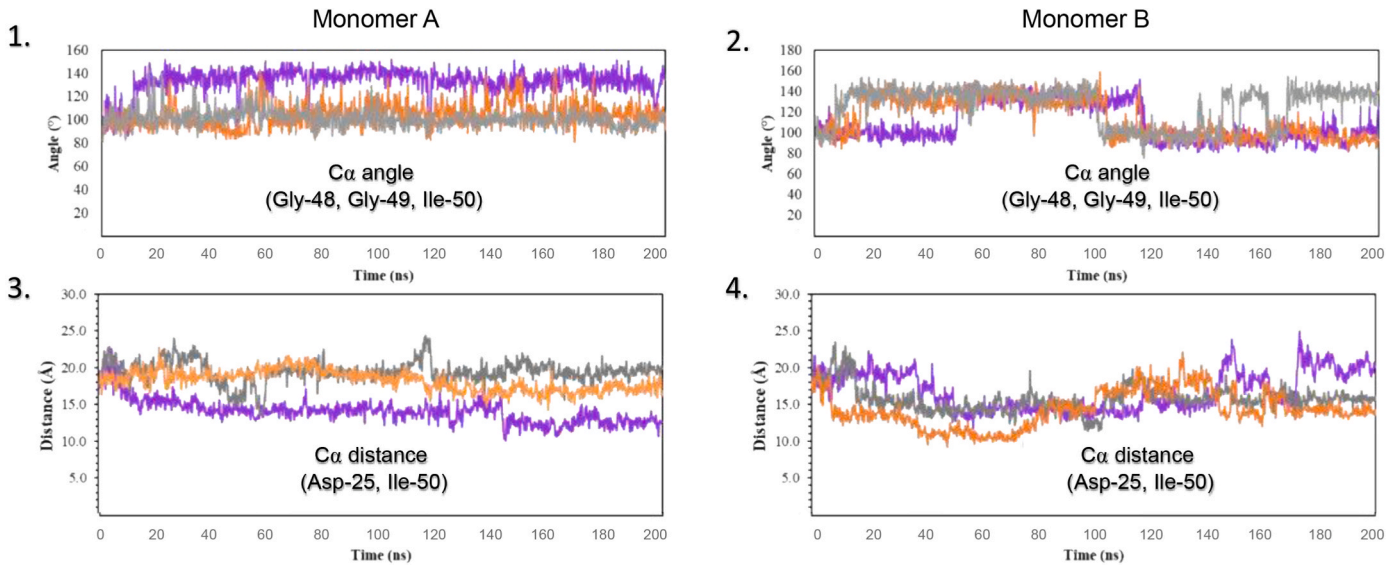


Fig. 2. Flap tip angle and flap conformations of WT PR (purple), N37T↑V (orange) PR and N37T↑V^{+10} PR (grey). Flap tip angles were measured as the angle between the Cα atoms of Gly-48, Ile-49, and Gly-50. Flap conformations were monitored by measuring the distance between the Cα atoms of Asp-25 and Ile-50. (For interpretation of the references to colour in this figure legend, the reader is referred to the Web version of this article.)

interatomic Asp25-Ile50 distance of <17 Å. Notably, the same monomer of both N37T↑V PR and N37T↑V^{+10} PR exhibited curling in of the flap tips at an angle of ~100° for the entire simulation, which corresponded with the flaps adopting the semi-open conformation (17–22 Å). Apo monomer B of WT PR initially adopted a curled-in flap tip with an angle of 100°, followed by curling out of the flap tip to ~140° and then finally reverting to 100°. The curling of the flap tips was, once again, mimicked in the conformation of the flaps. Here, the apo WT monomer initially adopted a semi-open conformation, followed by the closed conformation when the flap tips curled out towards ~140° and then moved back into the semi-open conformation when the flap tips curled in to 100°. These results show a strong correlation between the conformation (open, semi-open and closed) of the flaps and the curling of the flap tip residues (curling out and curling in), as previously suggested previously [18]. Monomer B of N37T↑V PR and N37T↑V^{+10} PR immediately adopted curled-out flap tip conformations (~140°) from 0 to 100 ns before curling inwards for 100–200 ns. Interestingly, the mutant PRs could adopt the curled-out flap tip conformation for extended periods of time compared to the WT PR. In monomer A, panel 1, the two variants represent similar flap dynamics in terms of C_α-angle compared to the WT. In monomer B, panel 2, in N37T↑V and N37T↑V^{+10} the flap dynamics are not comparable to each other. In monomer B, panel 2, N37T↑V^{+10} displays greater flap curling out and C_α-angle fluctuation in N37T↑V^{+10} compared to the WT and N37T↑V PR. Together, these findings may suggest that the N37T↑V^{+10} PR flaps are more likely to sample stable conformations over longer timescales than the WT PR. This is evidenced by the extended periods of sustained flap opening and curled-in flap tip conformations by the N37T↑V^{+10} PR. The background mutations in the hinges may increase the dynamics of the flaps. In contrast, mutations in the cantilever region may provide internal stability, enabling the flaps to maintain open and closed conformations for longer durations. This is important considering that altered flap dynamics and stability in the mutated PRs may affect decreased inhibitor susceptibility. Such mutations could allow the PR to exhibit increased flap opening and closing rates.

3.5. N37T↑V and N37T↑V^{+10} exhibit increased hinge and fulcrum region dynamics

The root-mean-square fluctuation (RMSF) quantifies the average deviation of the PR backbone atoms over the simulations. These analyses revealed significant differences in the dynamic behaviour of the apo N37T↑V PR and N37T↑V^{+10} PR compared to the apo WT PR. Specifically, the fulcrum and hinge regions of the N37T↑V and N37T↑V^{+10} mutants exhibited increased RMSF fluctuations, indicating increased flexibility in these regions (Fig. 3). The increased fluctuation in the fulcrum was noticeably more prominent in the N37T↑V^{+10} PR when compared to the N37T↑V PR. The N37T↑V^{+10} PR contains two mutations in the fulcrum region, I13V and G16E, which may alter the network of intramolecular interactions to increase the flexibility in this region.

Interestingly, while the hinge regions of N37T↑V and N37T↑V^{+10} were more dynamic, the cantilever region was found to be more stable for N37T↑V^{+10} compared to WT and N37T↑V, as indicated by a reduced RMSF in this region (Fig. 3 and Table S2). This finding contrasted with a previous study where it was found that the I13V mutation increased the flexibility of the cantilever region [18]. The difference is most likely due to several additional secondary mutations present in the cantilever region of the N37T↑V^{+10} protease; namely, D60E, D61E, I62V, L63P, and V77I. Naturally occurring polymorphisms between subtype B and subtype C PR, such as L63P, have been shown to affect the conformational flexibility of the HIV-1 protease, with L63P increasing the rigidity of the subtype B PR [29]. Residues 13, 62, 63, 77 and 89 are part of the twenty amino acids comprising the hydrophobic core of the PR [19]. The hydrophobic core plays a critical role in the flexibility and conformational changes of the PR and, specifically, the flap regions through the hydrophobic sliding mechanism [18,19,30]. Significant alterations in the hydrophobic sliding mechanism are postulated to result in reduced drug susceptibility. The presence of the ten background mutations may be essential for stabilising the cantilever in N37T↑V^{+10} PR in a manner that alters the intramolecular hydrophobic interactions of the PR. This stabilisation may be introduced to accommodate the wider conformation of the flap regions resulting from the increased dynamics of the hinges and fulcrum in the N37T↑V mutant. Overall, the results suggest that the N37T↑V PR and N37T↑V^{+10} PR mutants have altered dynamics in the hinge and cantilever regions, which are used to coordinate drug binding, which may, as a result, affect drug susceptibility.

3.6. Insertion mutations increase the dynamics of critical regions of the PR when complexed with PIs

The formation of stable interactions between the protease and

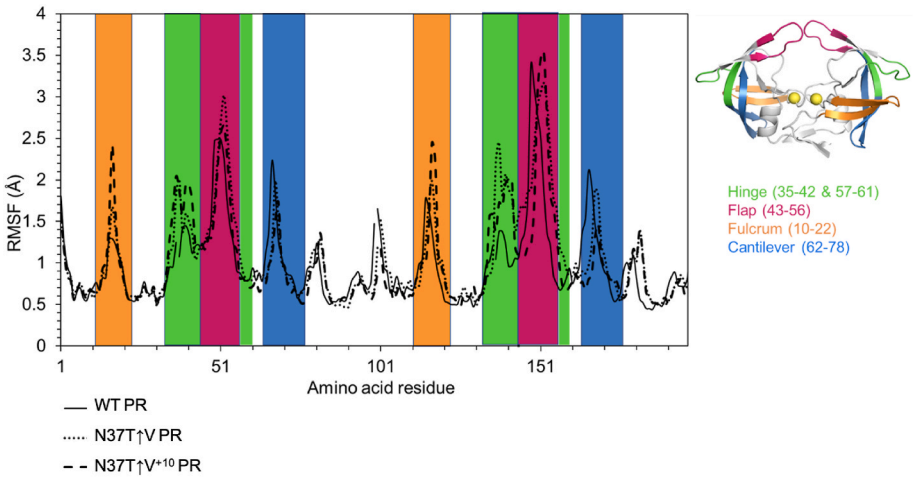


Fig. 3. The average RMSF of the regions in the apo WT PR, N37T↑V PR and N37T↑V^{+10} PR HIV-1 protease.

protease inhibitors is crucial for strong binding interactions required for sufficient inhibition to occur. Therefore, increased dynamics and flexibility of PR residues that contact PIs can weaken binding interactions and reduce drug susceptibility. Here, it was observed that distinct regions of the WT PR consistently exhibited decreased RMSF when in complex with several PIs: namely, ATV, DRV, FPV, NFV, RTV and TPV relative to the apo state (Fig. 4). However, for both the N37T↑V PR and N37T↑V^{+10} PR, the RMSF of the hinge and flap regions were significantly increased particularly when in a complex with ATV and DRV and, to a lesser extent, when in a complex with FPV and TPV. Increased flexibility in these regions (flap and hinges) relative to the WT PR may be significant when considering inhibition. As such, higher mobility of the flaps may lead to weaker or more transient interactions formed with PIs in the active site since PIs are inherently rigid and unable to accommodate perturbations in the active site.

3.7. *Cantilever tip angle contraction is essential for flap conformational changes*

Recently, Sherry et al., [18] highlighted the importance of cantilever tip angle contraction in facilitating conformational changes in flaps of the HIV-1 protease. While flap tip curling has traditionally been viewed as the primary mechanism for initiating flap movement, there is current evidence suggesting that the cantilever tip residues (Ile-66, Cys-67, Gly-68) may also play a critical role in regulating flap mobility. Previously, it has been shown that when the cantilever tip Cα angle is

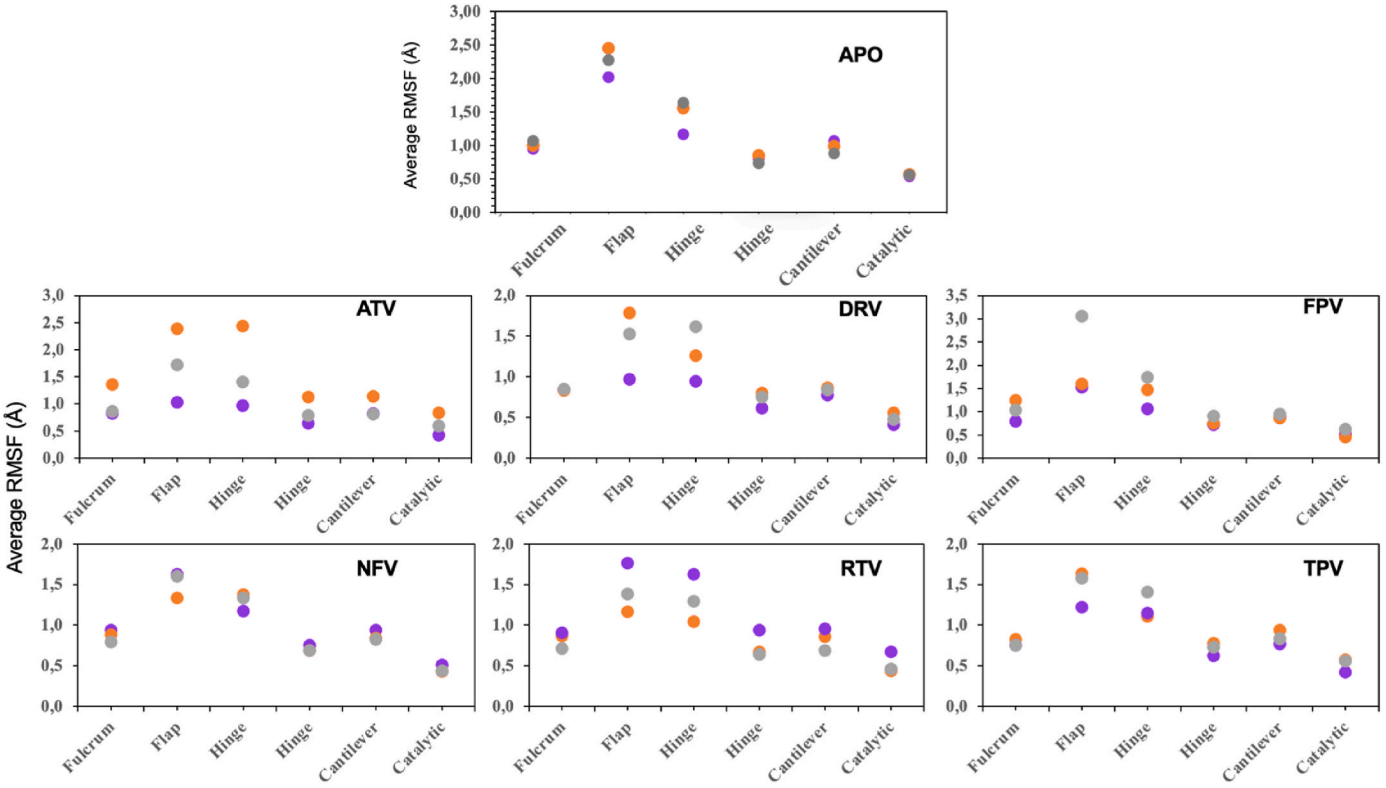


Fig. 4. Average RMSF of distinct regions of the WT PR, N37T↑V and N37T↑V^{+10} in the apo and drug-bound state. The distinct regions investigated include the fulcrum, flap, hinge, cantilever, and catalytic region. WT PR (purple), N37T↑V (orange) and N37T↑V^{+10} (grey). (For interpretation of the references to colour in this figure legend, the reader is referred to the Web version of this article.)

curled-in (≤100°) the flaps adopt a semi-open conformation and when this angle is curled-out (>100°), the flaps adopt the closed conformation [18]. In this study, the WT PR exhibited an average cantilever tip angle of 102.25°, indicative of a relaxed (curled-out) cantilever tip which correlated with a closed flap conformation (<17 Å) throughout the simulation (Fig. 5). In contrast, the N37T↑V and N37T↑V^{+10} mutants displayed cantilever tip angles of 96.73° and 94.76°, respectively, indicating a more curled-in conformation. As such, it is noteworthy that the flaps of the N37T↑V and N37T↑V^{+10} PRs were maintained in a semi-open flap conformation (17–22 Å). Previous NMR studies on HIV-1 PR have elucidated that the flap tips (residues 46–54) move from a closed conformation to an open conformation on a timescale considerably less than 10 ns [27,37,38]. This has further been shown to hold true in molecular dynamics simulations where the mean relaxation time of opening was shown to be ~8 ns which agrees with NMR studies [39]. Previous studies with shorter simulation timescales have confirmed that complete flap opening and closing occurs within these timescales [20,22,40]. Therefore, a 200 ns trajectory is sufficient to capture the relevant dynamics and to sample all the conformational states. These findings provide further evidence suggesting that cantilever tip angle contraction is a critical mechanism for regulating flap mobility and conformational change in HIV-1 PR. Therefore, the global dynamics of the PR must be considered when considering mechanisms of PR catalysis, inhibition, and resistance.

3.8. N37T↑V PR and N37T↑V^{+10} PR are less compact and do not fully enclose PIs

The flap regions of the PRs can adopt various conformational states that exist in equilibrium; however, inhibition via PIs should bring the flaps into a more stable and closed conformation. The stabilisation event results from the binding free energy associated with intermolecular interactions between the PR and the inhibitor [31]. Hence, non-active site mutations that increase the flexibility of the flaps when complexed to inhibitors may increase the dissociation constant of the complex. A phenomenon that has been characterised by resistance to Saquinavir [32]. The radius of gyration (R_g) is a measure of the degree of compactness of a protein during the MD simulation. A more dynamic system reflects an increased average R_g. Notably, the N37T↑V PR and N37T↑V^{+10} PR exhibit higher average R_g values than those of the WT PR when in the apo state and when bound to all six PIs tested (Fig. 6A). When comparing the N37T↑V PR and N37T↑V^{+10} PR, the latter more consistently exhibits increased R_g values compared to N37T↑V PR. This may suggest that the additional ten background mutations allow the N37T↑V^{+10} PR to sample a wider ensemble of dynamic states through increased internal rigidity. The R_g values indicate that the PIs were unable to fully "lock down" the mutant PRs as effectively as the WT PR. A similar trend is observed with the solvent accessible surface area (SASA) (Fig. 6B) for each PI, which is elevated in the mutant PR systems, particularly when in complex with ATV, DRV and RTV. These results are further supported by the observation that the closed flap conformation for the WT PR facilitates tighter interactions and, therefore, a decreased SASA. However, the semi-open conformation for the mutants results in less stable interactions, and as a result, this increase in dynamics is accompanied by an increase in the SASA. The increased solvent exposure would likely decrease the entropic favourability of burying the hydrophobic PIs in the active site cavity for a favourable interaction. As a result, this could potentially contribute to drug resistance.

Moreover, such alterations in the dynamics of the PR flaps and the increased solvent exposure of the PIs are likely to affect the quantity and quality of the intermolecular interactions formed. The number and strength of hydrogen bonds formed between the protease and inhibitors play a critical role in determining the binding affinity and specificity of the inhibitors (Rhee et al., 2010). Our analyses reveal that the N37T↑V PR and N37T↑V^{+10} PR form fewer hydrogen bonds with ATV, DRV, and RTV (Fig. S2). In these instances, the number of water-mediated contacts, or water bridges, formed in these complexes increases significantly. We have characterised a similar phenomenon in other PR

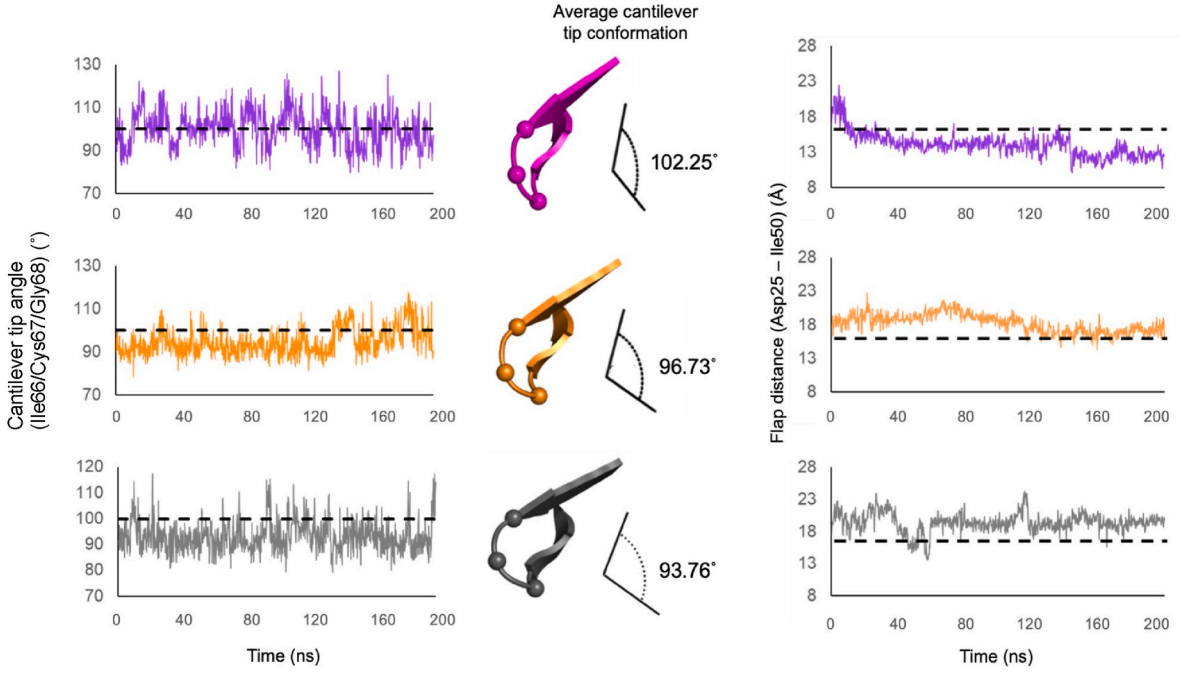


Fig. 5. HIV-1 PR cantilever tip contraction and flap conformational changes. Left: cantilever tip Cα angle between Ile-66, Cys-67, Gly-68. The broken line indicates the threshold between curled-in (≤100°) and curled-out (>100°) as per Sherry et al. [18]. Centre: the average cantilever tip conformation observed during molecular dynamics simulations. C_α atoms of Ile-66/Cys-67/Gly-68 are represented as spheres. Right: flap distance measured as the interatomic distance of the C_α from Ile-50 (flap) to Asp-25 (active site). The broken line indicates the threshold between closed (<17 Å) and semi-open (17–22 Å) flap conformations. The WT, N37T↑V and N37T↑V^{+10} are represented as purple, orange and grey, respectively. (For interpretation of the references to colour in this figure legend, the reader is referred to the Web version of this article.)

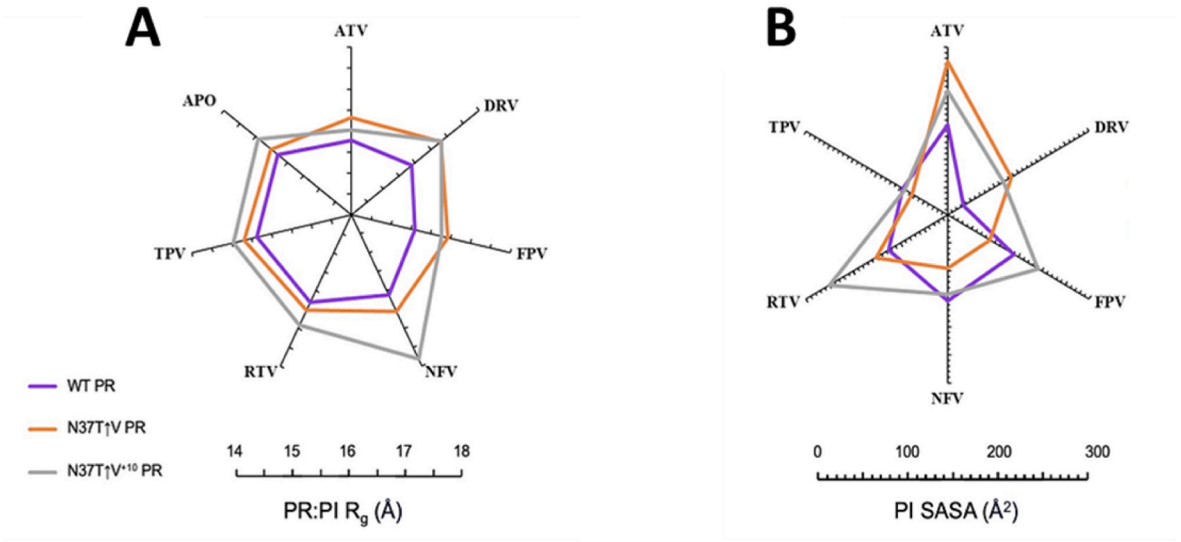


Fig. 6. A) radius of gyration (R_g) of WT PR (purple), N37T↑V PR (orange) and N37T↑V^{+10} PR (grey) B) PI solvent accessible surface area (SASA) and. The PI SASA was calculated for the PR in a complex with six inhibitors: ATV, DRV, FPV, NFV, RTV and TPV. The R_g values were calculated for the same six and apo PR systems. (For interpretation of the references to colour in this figure legend, the reader is referred to the Web version of this article.)

variants containing non-active site mutations [18]. We postulate that the increased flexibility of the flaps causes the inhibitor to be beyond hydrogen bonding distance with the active site Asp25/25′ residues when in contact with the flaps. This increased distance necessitates the formation of water bridges to maintain contact with the active site and the flaps simultaneously. Furthermore, the stability of water bridges compared to hydrogen bonds formed directly between the PR and inhibitor could diminish the enthalpic favourability of direct inhibitor binding to residues in the active site pocket. Therefore, the differences observed in the dynamics of the N37T↑V PR flaps and N37T↑V^{+10} PR may decrease inhibitor susceptibility by simultaneously decreasing the entropic and enthalpic favourability of inhibitor binding.

3.9. Alteration in intramolecular salt bridge formation

The HIV PR contains several structurally significant salt bridges involving residues of the flap and hinge regions of the PR comprising the following residue pairs: Lys-20/Glu-34, Asp-30/Lys-45, and Glu-35/Arg-57 and Lys-43/Asp-60 (Fig. S2). These salt bridges have been shown to play an essential role in the dynamics of the flap regions [20,33,34]. Furthermore, changes in the strength and occurrence of salt bridges in and surrounding the flaps have been hypothesised to play a role in drug resistance [20,35]. Analyses of the apo and drug-bound complexes of the N37T↑V PR and N37T↑V^{+10} PR revealed interesting changes in the interatomic distances of several salt bridges. Specifically, an increased interatomic distance was observed for two "anchoring" salt bridges, Asp30/Lys45 and Lys20/Glu34, in both mutant PRs in the apo state and complexed with all six PIs (Fig. S3). The Lys20/Glu34 salt bridge anchors the hinge region to the fulcrum region, while Asp30/-Lys45 anchors the flap region to the active site. An increase in the average interatomic distance observed in these anchoring salt bridges will likely result in increased dynamics of the flap and hinge regions relative to the WT PR. Conversely, salt bridges between the flap and hinge region exhibited a decreased average interatomic distance in the mutant PRs (Fig. S4). The Lys43/Asp60 and Lys20/Glu35 salt bridges connect the hinge region to the flap region (Fig. S4). The strengthening of these interactions may provide increased receptivity of the flap regions to alterations in the dynamics of the hinges. It is well understood that the Glu35/Arg57 salt bridge plays a crucial role in maintaining the closed conformation of the flaps [20,34]. Therefore, it could be postulated that changes in the interatomic distances of several other key salt bridges could significantly alter the flap dynamics of the PR. As such, future work should investigate the importance of these specific salt bridges involving the flap and hinge regions of the PR.

3.10. Relevance of current HIV-1 protease variants with respect to work on mutational effects in other HIV-1 proteases

It has been hypothesised that mutations throughout the protease alter the protein conformational ensemble and can shift the dynamic equilibrium towards substrate processing and away from inhibitor binding [44]. Resistance is thought to emerge when the balance of molecular recognition and flap dynamics favours that of substrate binding over inhibition. Thus, to elucidate the underlying mechanisms of drug resistance, molecular dynamics analyses are essential. Indeed, molecular dynamics simulations have been shown to illustrate that the conformational dynamics of drug-resistant PR variants are different from that of the WT PR [41]. Non-active site mutations were initially perceived as contributors to overall protein stability in drug-resistant protease variants. However, these mutations may have significant effects on the active site and have been shown to play a substantial role in drug resistance [36,42]. Interestingly, a study combining machine learning with molecular dynamics simulations illustrated that resistant PR variants converged to the same molecular feature phenotypes suggesting that drug resistance is mediated through conserved and specific mechanisms that are independent of the particular sites or types of sequence polymorphisms [43].

4. Conclusion

The dynamics of the hinge and flap regions of the PR play an essential role in the successful function and inhibition of the enzyme. Non-active site mutations that alter the flexibility of the hinge and flap regions may contribute to drug resistance by altering the dynamics of critical regions of the HIV-1 PR. Novel PR variants with hinge region insertions have been increasingly characterised in literature [11,20,21]. Understanding the mechanism of action of hinge region insertions may shed light on how such mutations could lead to reduced drug susceptibility.

Our study aimed to investigate how background mutations of N37T↑V^{+10} PR augment the effect of the insertion and substitution mutation in the hinge region of the N37T↑V PR. The insertion mutation and non-active site polymorphisms result in significant changes in the

flap dynamics and flexibility of the enzyme (Figs. 2 and 3). The apo mutant PRs adopt a semi-open conformation with wider flap conformations, while the apo WT PR is more compact and adopts a more closed conformation. The hinge region mutations present in N37T↑V PR introduce significant flexibility, which translates to more dynamic flaps. However, the excessive flexibility of the hinges may be detrimental without the stabilising effects of the background mutations present in N37T↑V^{+10} PR. We have also observed more flexible hinges and fulcrum in N37T↑V and N37T↑V^{+10} PR, while the cantilever region showed reduced flexibility. These conformational changes were also associated with an increase in the curling of the cantilever Ile-67/Cys-68/Gly-69 tip residues, correlated with a more open flap conformation in the mutated PR variants (Fig. 5).

These data also indicate that the flap regions of the N37T↑V PR and N37T↑V^{+10} PR fluctuate more readily when in complex with certain PIs in comparison to the WT PR (Fig. 4). In addition, the mutant PRs display higher R_g values when drug-bound and, in some instances, the PIs were more solvent-exposed than the corresponding WT PR complexes (Fig. 6). The mutations in N37T↑V PR and N37T↑V^{+10} PR caused increased solvent exposure of several PIs, suggesting that the complex formation would be less entropically favourable. Moreover, the mutant proteases formed fewer hydrogen bonds with inhibitors and, instead, formed less stable water bridges. This is likely a result of the ability of the mutated PRs to adopt wider flap conformations for more extended periods (Fig. 2).

In conclusion, we postulate that the insertion mutation (↑V) in N37T↑V PR and the additional background mutations in N37T↑V^{+10} PR result in less favourable binding of inhibitors both enthalpically and entropically. The increased flap dynamics and reduced drug binding interactions introduced by these non-active site mutations likely lead to resistance by altering the PR dynamics. These results have important implications for understanding how non-active site mutations may lead to the development of drug resistance.

CRediT authorship contribution statement

Tshele Mokhantso: Writing – review & editing, Writing – original draft, Validation, Methodology, Investigation, Formal analysis. **Dean Sherry:** Writing – review & editing. **Roland Worth:** Writing – review & editing. **Ramesh Pandian:** Writing – review & editing, Visualization, Validation, Software, Methodology, Formal analysis. **Ikechukwu Achilonu:** Writing – review & editing, Visualization, Validation, Supervision, Software, Methodology, Investigation, Formal analysis. **Yasien Sayed:** Writing – review & editing, Visualization, Validation, Supervision, Software, Resources, Project administration, Methodology, Investigation, Funding acquisition, Formal analysis, Data curation, Conceptualization.

Declaration of competing interest

The authors declare the following financial interests/personal relationships which may be considered as potential competing interests:

Yasien Sayed reports financial support was provided by University of the Witwatersrand Johannesburg School of Molecular and Cell Biology. If there are other authors, they declare that they have no known competing financial interests or personal relationships that could have appeared to influence the work reported in this paper.

Data availability

Data will be made available on request.

Acknowledgements

The research reported in this publication was supported by the National Research Foundation Competitive Support for Rated Researchers [CSRP170428229183] to Yasien Sayed. The views and opinions expressed are those of the authors and do not necessarily represent the official views of the NRF. The authors would like to thank Dr Gillian Hunt and Ms Johanna Ledwaba for identifying the variant protease sequence used in this study. The authors declare that there are no competing interests associated with the manuscript.

Appendix A. Supplementary data

Supplementary data to this article can be found online at https://doi.org/10.1016/j.jmgm.2024.108850.

References

[1] C. Debouck, The HIV-1 protease as a therapeutic target for AIDS, AIDS Res. Hum. Retrovir. 8 (1992) 153–164, https://doi.org/10.1089/aid.1992.8.153.
[2] C. Bossard, B. Schramm, S. Wanjala, L. Jain, G. Mucinya, V. Opollo, L. Wiesner, G. Van Cutsem, E. Poulet, E. Szumilin, T. Ellman, D. Maman, High prevalence of NRTI and NNRTI drug resistance among ART-experienced, hospitalized inpatients, JAIDS J. Acqu. Immu. Defici. Syndrom. (2021), https://doi.org/10.1097/QAI.0000000000002689.
[3] E.L. Murphy, A.C. Collier, L.A. Kalish, S.F. Assmann, M.F. Para, T.P. Flanigan, P. N. Kumar, L. Mintz, F.R. Wallach, G.J. Nemo, Highly active antiretroviral therapy decreases mortality and morbidity in patients with advanced HIV disease, Ann. Intern. Med. 135 (2001) 17, https://doi.org/10.7326/0003-4819-135-1-200107030-00005.
[4] R. Detels, Effectiveness of potent antiretroviral therapy on time to AIDS and death in men with known HIV infection duration, JAMA 280 (1998) 1497, https://doi.org/10.1001/jama.280.17.1497.
[5] R.W. Shafer, J.M. Schapiro, HIV-1 drug resistance mutations: an updated framework for the second decade of HAART, AIDS Rev. 10 (2008) 67–84.
[6] D. Vlahov, N. Galai, M. Safaeian, S. Galea, G.D. Kirk, G.M. Lucas, T.R. Sterling, Effectiveness of highly active antiretroviral therapy among injection drug users with late-stage human immunodeficiency virus infection, Am. J. Epidemiol. 161 (2005) 999–1012, https://doi.org/10.1093/aje/kwi133.
[7] H. Ohtaka, A. Velázquez-Campoy, D. Xie, E. Freire, Overcoming drug resistance in HIV-1 chemotherapy: the binding thermodynamics of Amprenavir and TMC-126 to wild-type and drug-resistant mutants of the HIV-1 protease, Protein Sci. 11 (2002) 1908–1916, https://doi.org/10.1110/ps.0206402.
[8] P.O. Bessong, Polymorphisms in HIV-1 subtype C proteases and the potential impact on protease inhibitors, Trop. Med. Int. Health 13 (2008) 144–151, https://doi.org/10.1111/j.1365-3156.2007.01984.x.
[9] Z. Liu, X. Huang, L. Hu, L. Pham, K.M. Poole, Y. Tang, B.P. Mahon, W. Tang, K. Li, N.E. Goldfarb, B.M. Dunn, R. McKenna, G.E. Fanucci, Effects of hinge-region natural polymorphisms on human immunodeficiency virus-type 1 protease structure, dynamics, and drug pressure evolution, J. Biol. Chem. 291 (2016) 22741–22756, https://doi.org/10.1074/jbc.M116.747568.
[10] D. Sherry, R. Pandian, Y. Sayed, Non-active site mutations in the HIV protease: diminished drug binding affinity is achieved through modulating the hydrophobic sliding mechanism, Int. J. Biol. Macromol. 217 (2022) 27–41, https://doi.org/10.1016/j.ijbiomac.2022.07.033.
[11] S. Venkatachalam, N. Murlidharan, S.R. Krishnan, C. Ramakrishnan, M. Setshedi, R. Pandian, D. Barh, S. Tiwari, V. Azevedo, Y. Sayed, M.M. Gromiha, Understanding drug resistance of wild-type and L38HL insertion mutant of HIV-1 C protease to Saquinavir, Genes 14 (2023) 533, https://doi.org/10.3390/genes14020533.
[12] S. Eche, A. Kumar, N. Sonela, M.L. Gordon, Acquired HIV-1 protease conformational flexibility associated with Lopinavir failure may shape the outcome of Darunavir therapy after antiretroviral therapy switch, Biomolecules 11 (2021) 489, https://doi.org/10.3390/biom11040489.
[13] S. Mosebi, L. Morris, H.W. Dirr, Y. Sayed, Active-site mutations in the South African human immunodeficiency virus type 1 subtype C protease have a significant impact on clinical inhibitor binding: kinetic and thermodynamic study, J. Virol. 82 (2008) 11476–11479, https://doi.org/10.1128/JVI.00726-08.
[14] A. Velazquez-Campoy, S. Vega, E. Freire, Amplification of the effects of drug resistance mutations by background polymorphisms in HIV-1 protease from African subtypes, Biochemistry 41 (2002) 8613–8619, https://doi.org/10.1021/bi020160i.
[15] J.C. Clemente, R.E. Moose, R. Hemrajani, L.R.S. Whitford, L. Govindasamy, R. Reutzel, R. McKenna, M. Agbandje-McKenna, M.M. Goodenow, B.M. Dunn, Comparing the accumulation of active- and nonactive-site mutations in the HIV-1 protease, Biochemistry 43 (2004) 12141–12151, https://doi.org/10.1021/bi049459m.
[16] J.D. Bloom, L.I. Gong, D. Baltimore, Permissive secondary mutations enable the evolution of influenza oseltamivir resistance, Science 328 (1979) (2010) 1272–1275, https://doi.org/10.1126/science.1187816.
[17] N.E. Goldfarb, M. Ohanessian, S. Biswas, T.D. McGee, B.P. Mahon, D.A. Ostrov, J. Garcia, Y. Tang, R. McKenna, A. Roitberg, B.M. Dunn, Defective hydrophobic sliding mechanism and active site expansion in HIV-1 protease drug resistant variant Gly48Thr/Leu89Met: mechanisms for the loss of Saquinavir binding potency, Biochemistry 54 (2015) 422–433, https://doi.org/10.1021/bi501088e.

[18] D. Sherry, R. Worth, Z.S. Ismail, Y. Sayed, Cantilever-centric mechanism of cooperative non-active site mutations in HIV protease: implications for flap dynamics, J. Mol. Graph. Model. 106 (2021) 107931, https://doi.org/10.1016/j.jmgm.2021.107931.
[19] J.E. Foulkes-Murzycki, W.R.P. Scott, C.A. Schiffer, Hydrophobic sliding: a possible mechanism for drug resistance in human immunodeficiency virus type 1 protease, Structure 15 (2007) 225–233, https://doi.org/10.1016/j.str.2007.01.006.
[20] J. Zondagh, V. Balakrishnan, I. Achilonu, H.W. Dirr, Y. Sayed, Molecular dynamics and ligand docking of a hinge region variant of South African HIV-1 subtype C protease, J. Mol. Graph. Model. 82 (2018) 1–11, https://doi.org/10.1016/j.jmgm.2018.03.006.
[21] A. Williams, A. Basson, I. Achilonu, H.W. Dirr, L. Morris, Y. Sayed, Double trouble? Gag in conjunction with double insert in HIV protease contributes to reduced DRV susceptibility, Biochem. J. 476 (2019) 375–384, https://doi.org/10.1042/BCJ20180692.
[22] Z. Sheik Ismail, R. Worth, S. Mosebi, Y. Sayed, HIV protease hinge region insertions at codon 38 affect enzyme kinetics, conformational stability and dynamics, Protein J. (2023), https://doi.org/10.1007/s10930-023-10132-6.
[23] S. Maseko, E. Padayachee, S. Maphumulo, T. Govender, Y. Sayed, G. Maguire, J. Lin, T. Naicker, S. Baijnath, K.H. Gerhardus, Kinetic and thermodynamic characterisation of HIV-protease inhibitors against E35D↑G↑S mutant in the South African HIV-1 subtype C protease, J. Enzym. Inhib. Med. Chem. 34 (2019) 1451–1456, https://doi.org/10.1080/14756366.2019.1636234.
[24] R.A. Laskowski, M.W. MacArthur, D.S. Moss, J.M. Thornton, PROCHECK: a program to check the stereochemical quality of protein structures, J. Appl. Crystallogr. 26 (1993) 283–291, https://doi.org/10.1107/S0021889892009944.
[25] H. Okumura, S.G. Itoh, Y. Okamoto, Explicit symplectic integrators of molecular dynamics algorithms for rigid-body molecules in the canonical, isobaric-isothermal, and related ensembles, J. Chem. Phys. 126 (2007), https://doi.org/10.1063/1.2434972.
[26] A. Wlodawer, J. Vondrasek, Inhibitors OF HIV-1 PROTEASE: a major success of structure-assisted drug design, Annu. Rev. Biophys. Biomol. Struct. 27 (1998) 249–284, https://doi.org/10.1146/annurev.biophys.27.1.249.
[27] W.R.P. Scott, C.A. Schiffer, Curling of flap tips in HIV-1 protease as a mechanism for substrate entry and tolerance of drug resistance, Structure 8 (2000) 1259–1265, https://doi.org/10.1016/S0969-2126(00)00537-2.
[28] A.L. Perryman, J.-H. Lin, J.A. McCammon, HIV-1 protease molecular dynamics of a wild-type and of the V82F/I84V mutant: possible contributions to drug resistance and a potential new target site for drugs, Protein Sci. 13 (2004) 1108–1123, https://doi.org/10.1110/ps.03468904.
[29] J.D. Carter, E.G. Gonzales, X. Huang, A.N. Smith, I.M.S. de Vera, P.W. D'Amore, J. R. Rocca, M.M. Goodenow, B.M. Dunn, G.E. Fanucci, Effects of PRE and POST therapy drug-pressure selected mutations on HIV-1 protease conformational sampling, FEBS Lett. 588 (2014) 3123–3128, https://doi.org/10.1016/j.febslet.2014.06.051.
[30] D.A. Ragland, E.A. Nalivaika, M.N.L. Nalam, K.L. Prachanronarong, H. Cao, R. M. Bandaranayake, Y. Cai, N. Kurt-Yilmaz, C.A. Schiffer, Drug resistance conferred by mutations outside the active site through alterations in the dynamic and structural ensemble of HIV-1 protease, J. Am. Chem. Soc. 136 (2014) 11956–11963, https://doi.org/10.1021/ja504096m.
[31] M.J. Todd, E. Freire, The effect of inhibitor binding on the structural stability and cooperativity of the HIV-1 protease, Proteins 36 (1999) 147–156, https://doi.org/10.1002/(sici)1097-0134(19990801)36:2<147::aid-prot2>3.0.co;2-156.
[32] B. Maschera, G. Darby, G. Palú, L.L. Wright, M. Tisdale, R. Myers, E.D. Blair, E. S. Furfine, Human immunodeficiency virus, J. Biol. Chem. 271 (1996) 33231–33235, https://doi.org/10.1074/jbc.271.52.33231.
[33] D.M. York, T.A. Darden, L.G. Pedersen, M.W. Anderson, Molecular dynamics simulation of HIV-1 protease in a crystalline environment and in solution, Biochemistry 32 (1993) 3196, https://doi.org/10.1021/bi00063a035, 3196.
[34] M.A. Swairjo, E.M. Towler, C. Debouck, S.S. Abdel-Meguid, Structural role of the 30's loop in determining the ligand specificity of the human immunodeficiency virus protease, Biochemistry 37 (1998) 10928–10936, https://doi.org/10.1021/bi980784h.
[35] P. Naicker, P. Seele, H.W. Dirr, Y. Sayed, F99 is critical for dimerization and activation of South African HIV-1 subtype C protease, Protein J. 32 (2013) 560–567, https://doi.org/10.1007/s10930-013-9517-y.
[36] S.Y. Rhee, J. Taylor, W.J. Fessel, D. Kaufman, W. Towner, P. Troia, P. Ruane, J. Hellinger, V. Shirvani, A. Zolopa, R.W. Shafer, HIV-1 protease mutations and protease inhibitor cross-resistance, Antimicrob. Agents Chemother. 54 (10) (2010) 4253–4261, https://doi.org/10.1128/AAC.00574-10.
[37] R. Ishima, D.I. Freedverg, Y.-X. Wang, J.M. Louis, D.A. Torchia, Flap opening and dimer-interface flexibility in the free and inhibitor-bound HIV protease, and their implications for function, Structure 7 (1999) 1047–1055, https://doi.org/10.1016/s0969-2126(99)80172-5.
[38] E. Katoh, J.M. Lou, T. Yamazaki, A.M. Gronenborn, D.A. Torchia, R. Ishima, A solution NMR study of the binding kinetics and the internal dynamics of an HIV-1 protease-substrate complex, Protein Sci. (2009) 1047–1055, https://doi.org/10.1110/ps.0300703.
[39] S.K. Sadiq, G. De Fabritis, Explicit solvent dynamics and energetics of HIV-1 protease flap opening and closing, Proteins 78 (2010) 2873–2885, https://doi.org/10.1002/prot.22806.
[40] S. Venkatachalam, N. Murlidharan, S.R. Krishnan, C. Ramakrishnan, M. Setshedi, R. Pandian, D. Barh, S. Tiwari, V. Azevedo, Y. Sayed, M.M. Gromiha, Understanding drug resistance of wild-type and L38HL insertion mutant of HIV-1 C protease to Saquinavir, Genes 14 (2023) 533, https://doi.org/10.3390/genes14020533.
[41] M. Souffrant, X.-Q. Yao, D. Hamelberg, Evolving mutational buildup in HIV-1 protease shifts conformational dynamics to gain drug resistance, J. Chem. Inf. Model. 63 (2023) 3892–3902, https://doi.org/10.1021/acs.jcim.3c00535.
[42] D.A. Ragland, T.W. Whitfield, S.K. Lee, R. Swanstrom, K.B. Zeldovich, N. Kurt-Yilmaz, C.A. Schiffer, Elucidating the interdependence of drug resistance from combinations of mutations, J. Chem. Theor. Comput. 13 (2017) 5671–5682, https://doi.org/10.1021/acs.jctc.7b00601.
[43] F. Leidner, N. Kurt-Yilmaz, C.A. Schiffer, Decifering complex mechanisms of resistance and loss of potency through coupled molecular dynamics and machine learning, J. Chem. Theor. Comput. 17 (2021) 2054–2064, https://doi.org/10.1021/acs.jctc.0c01244.
[44] D. Sherry, R. Worth, Y. Sayed, Elasticity-associated functionality and inhibition of HIV protease, Adv. Exp. Med. Biol. (2022) 79–108, https://doi.org/10.1007/5584_2021_655.
[45] H.A. Lockhat, J.R.A. Silva, C.N. Alvez, T. Govender, J. Lameira, G.E.M. Maguire, Y. Sayed, H.G. Kruger, Binding free energy calculations of nine-fda approved protease inhibitors against HIV-1 subtype C I36TT containing 100 amino acids per monomer, Chem. Biol. Drug Des. 87 (2016) 487–498, https://doi.org/10.1111/cbdd.12690.
[46] G.M. Ko, A.S. Reddy, S. Kumar, B.A. Baileyand R Garg, Computational analysis of HIV-1 protease protein binding pockets, J. Chem. Inf. Model. 50 (2010) 1759–1771, https://doi.org/10.1021/ci100200u.
[47] A.K. Halder, B. Honarparvar, Molecular alteration in drug susceptibility against subtype B and C-SA HIV-1 proteases: MD study, Struct. Chem. 30 (2019) 1715–1727, https://doi.org/10.1007/s11224-019-01305-0.